A semiparametric step-stress competing risk model

Aman Prakash[1], Debashis Samanta[2*], Raj Kamal Maurya[1], Debasis Kundu[3]

[1]*Department of Mathematics, National Institute of Technology Surat, Surat, Gujarat, India*
[2]*Department of Mathematics and Statistics, Aliah University, Kolkata, West Bengal, India*
[3]*Department of Mathematics and Statistics, Indian Institute of Technology Kanpur, Kanpur, India*

*Corresponding author: deba007.stat@gmail.com

Abstract: This article proposes a flexible semiparametric framework for a simple step-stress accelerated life-testing experiment in the presence of two independent competing risks. The stress is assumed to change from an initial level to a higher level at a pre-specified time. Instead of assuming a single parametric form for the hazard function over each stress level, we divide the time axis within each stress level into several sub-intervals using cut points. Within each sub-interval, the cause-specific hazard rates are assumed as a piecewise monotone hazard function. This framework provides a good approximation to a broad class of hazard functions and allows the failure rate to exhibit increasing, decreasing, or constant patterns over time, depending on the underlying failure mechanism. It is a natural generalization of the piecewise constant hazard function. The piecewise constant hazard function can be obtained as a special case. We develop both classical and Bayesian inference procedures for the proposed framework. Maximum likelihood estimates of the model parameters and their asymptotic confidence intervals are obtained. Bayesian inference is carried out by assuming a flexible prior distribution. We obtained the Bayes estimates and the associated credible intervals of the model parameters under squared error loss function. The performance of the proposed estimators has been examined through an extensive simulation study. A real-life dataset is analyzed to illustrate the practical applicability and effectiveness of the proposed methodology. In practice, the locations of the cut points are often unknown and play a crucial role in model performance. So, we address this issue by determining the cut points using a non-homogeneous Poisson process model for the real dataset.

Keywords: Accelerated life testing, Piecewise monotone hazard function, Competing risk, Step-stress models, Maximum likelihood estimation, Bayesian estimation

1 Introduction

In recent years, advances in manufacturing technology and quality control have led to the production of highly reliable products. While this improvement is desirable from an engineering perspective, it creates practical difficulties for reliability assessment. Under normal operating conditions, failures may occur very infrequently, making conventional life-testing experiments time-consuming, expensive, and often infeasible within a reasonable experimental duration. As a result, obtaining sufficient failure information using traditional testing methods becomes challenging. Therefore, accelerated life testing (ALT) has emerged as an essential tool in reliability analysis for highly reliable products. In ALT, test units are run under higher stress levels, such as increased temperature, voltage, or load, so that failures happen fast. This approach helps experimenters to obtain useful lifetime data in a shorter time

and makes it possible to assess the reliability of products under normal usage conditions. Once data are collected from an ALT experiment, it is extrapolated to estimate various reliability characteristics under normal operating conditions. Among the various ALT schemes, step-stress accelerated life testing has attracted considerable attention due to its practical relevance and experimental flexibility. In step-stress ALT, units are initially employed under a lower stress level, and the stress is increased at prefixed time points or a fixed number of failures during the experiment. This staged escalation of stress more closely reflects real-world operating environments. The simplest form of this framework involves only two stress levels, commonly referred to as a simple step-stress model. More complex experiments, however, may involve multiple stress changes, leading to multi-step stress models. Notable references in the area of ALT models include Bagdonavicius et al. (2004)[1], Miller and Nelson (2009)[2], and Meeker and Escobar (2021)[3].

Several statistical models have been developed to analyze the obtained data from simple and multiple-step stress ALT experiments. Among these, the cumulative exposure model, initially proposed by Sedyakin (1966)[4], is one of the earliest and most commonly applied approaches, as it accounts for the accumulated effect of stress over time. Another important model is the tampered failure rate model, introduced by Bhattacharyya and Soejoeti (1989)[5], which allows the failure rate to change after a stress level is altered. More recently, Kateri and Kamps (2015)[6] proposed a failure rate–based modeling framework that provides additional flexibility for characterizing the effects of step-stress changes on the failure mechanism. For a detailed and systematic discussion of these models, along with other available approaches in the step-stress ALT literature, readers are referred to the monograph by Kundu and Ganguly (2017)[7].

Parametric lifetime models typically impose a single functional form of the hazard function over the entire time frame, which restricts it to follow a specific pattern such as monotone increasing, decreasing, or constant. These assumptions are convenient from a modeling perspective, but it is restrictive in practical survival studies, particularly when the underlying failure mechanism changes over the time. In such situations, enforcing a global hazard rate may lead to model misspecification and biased inference. To overcome with this limitation, semiparametric approaches have been discussed in the literature, most commonly through the use of piecewise-constant hazard functions defined over pre-specified time intervals (see Murphy (1996)[8], Balakrishnan et al. (2016)[9], Samanta and Kundu (2023)[10] and Ganguly et al. (2024)[11]). These models allow the hazard rate to vary across intervals rather than requiring a fixed hazard function, which offers greater flexibility while retaining interpretability. However, if the hazard rate is assumed to be constant within each interval, it may not adequately capture gradual aging effects or time-dependent failure patterns.

Therefore, in the present work, we adopt a semiparametric strategy by modeling the hazard function across a finite number of time intervals. The proposed framework uses a piecewise monotone hazard function (PMHF) model. Within each subinterval, the hazard rate is monotonically increasing, decreasing, or constant depending on the value of the shape parameter. As a result, the proposed model naturally generalizes the widely used piecewise constant hazard function (PCHF) model. In particular, the PCHF model is obtained as a special case when the shape parameter is equal to one in each stress level. By allowing monotonic hazard behavior within subintervals rather than enforcing constancy, the proposed approach provides greater flexibility for capturing gradual aging effects and time-dependent failure mechanisms while retaining analytical tractability. This approach preserves the parametric structure locally and avoids the restrictive assumption of a globally fixed hazard rate. Recently, Pal et al. (2025)[12] and Prajapati and Kundu (2025)[13] have explored semiparametric inference by adopting PCHF rate models under Type-I and progressive censoring schemes, respectively. These studies demonstrate the usefulness of semiparametric formulations in relaxing global hazard assumptions, while maintaining analytical tractability. Compared to PCHF models, the proposed PMHF model offers several advantages. First, it avoids the unrealistic assumption of a constant failure rate within each interval and allows for smooth monotonic changes in risk. Second, it preserves a clear

parametric interpretation within each subinterval. Third, the model remains computationally feasible even with multiple cut points, while providing improved adaptability to complex failure patterns commonly observed in step-stress accelerated life testing experiments. These features make the proposed framework particularly suitable for applications where failure mechanisms evolve gradually over time and across stress levels.

In many life-testing experiments, experimental units may fail due to more than one underlying cause, giving rise to competing risks data, where each observation consists of both the failure time and the associated cause of failure. In this study, the analysis of competing risks data is carried out under the latent failure time framework introduced by Cox (1959)[14]. Under this formulation, each experimental unit is assumed to be associated with a set of latent failure times corresponding to the causes of failure, and the observed lifetime is the minimum of these latent times. The cause of failure is determined by the risk that realizes first, while the remaining latent failure times remain unobserved. The analysis of competing risks data has been developed under parametric assumptions for cause-specific lifetime distributions, including the latent failure time framework proposed by Cox (1959)[14] and subsequent extensions by David and Moeschberger (1978)[15]. In the context of step-stress ALT, competing risks models have been investigated by several authors, including Beltrami (2015)[16], Balakrishnan and Han (2008)[17], Liu and Qiu (2011)[18], Zhang et al. (2016)[19], Samanta et al. (2019)[20] and others. Despite these advances, most existing step-stress competing risks models impose a single parametric hazard structure over the entire framework, which is restrictive. In this study, we consider a simple step-stress life-testing model with two independent competing causes of failures. To allow additional flexibility, the time axis under each stress level is partitioned into a finite number of pre-specified subintervals. For each stress level and failure cause, the lifetimes of units are assumed to follow a PMHF. We have assumed that the distribution is defined by a stress-specific shape parameter α_i $(i = 1, 2)$ and subinterval-specific scale parameters $\lambda_{k,r}$, where $k = 1, 2$ denotes the cause of failure and r indexes the corresponding subintervals. This proposed framework gives a semiparametric modeling based on a PMHF. To the best of our knowledge, the use of a PMHF for step-stress life testing in the presence of competing risks has not been explored in the literature. Furthermore, the proposed model is developed under Type-I censoring, where the experiment is terminated at a fixed time T, and the stress level is changed at a pre-specified time τ.

In this study, we have developed both classical and Bayesian inference procedures under the proposed semiparametric framework. A flexible failure-rate model is adopted to relate lifetime distributions corresponding to two different stress levels. Maximum likelihood estimation (MLE) and Bayesian estimation under squared error loss function, of the model parameters are derived, and their associated confidence and credible intervals are constructed. The performances of the proposed inferential procedures are evaluated through extensive simulation studies. Although the proposed methodology is presented for the case of two stress levels and two competing causes of failure for ease of presentation, but the framework can be easily extended to accommodate more than two stress levels or competing risks in a similar manner. Furthermore, to demonstrate the practical applicability of the proposed framework, we have illustrated its use on a real-life AIDS dataset with two competing failure causes under Type-I censoring. The selection of cut points plays an important role in the proposed modeling framework. In this study, following the approach of Samanta and Kundu (2023)[10], we assume that the cut points occur according to a non-homogeneous Poisson process with a power-law intensity function. Under this assumption, the cut points are determined using the MLEs of the event times in the NHPP. To illustrate the applicability of the proposed method, a real dataset is analyzed.

The rest of the paper is organized as follows. Section 2 presents the model description of the proposed semiparametric framework. Maximum likelihood estimation of the model parameters, along with the associated asymptotic confidence interval, is discussed in Section 3. Bayesian inference for the model parameters is developed in Section 4. An extensive simulation study is conducted in Section 5 to evaluate the performance of the proposed methods. In Section 6, the applicability of the proposed

framework is illustrated using a real data set. Also discussed the process of selecting the number and location of the cut points. Finally, concluding remarks are provided in Section 7.

2 Model Description

Step-stress ALT experiments are designed to accelerate failure occurrence by exposing test units to increasing levels of stress over time. In such settings, the underlying failure mechanism may evolve across different phases of the experiment, making it inadequate to assume a single global hazard structure. A flexible hazard-based modelling approach is therefore desirable to capture variations in failure behavior induced by stress changes and temporal effects. In this framework, we have assumed that at the beginning of the experiment, n identical and independent test units are placed under the initial stress level s_1. The stress level is elevated to a higher level s_2 at a pre-specified time point τ, and the experiment is terminated at a fixed time $T > \tau$. We have considered two independent causes of failure, and each unit is subject to failure from one of the two competing causes. The competing risks in this study are developed within the latent failure-time paradigm. To allow sufficient flexibility in modeling of failure mechanisms under varying stress conditions, we adopt a semiparametric approach based on a PMHF model. To accommodate possible changes in the failure behavior over time, each stress level is further partitioned into a finite number of subintervals using a set of cut points. Specifically, the time interval $(0, \tau]$ corresponding to stress level s_1 is divided into M subintervals by cut points $0 = \tau_0 < \tau_1 < \cdots < \tau_M = \tau$. While the interval $(\tau, T]$ corresponding to stress level s_2 is divided into Q subintervals by $\tau = \gamma_0 < \gamma_1 < \cdots < \gamma_Q = T$. For notational convenience, we denote the complete collection of subintervals by $(a_r, b_r]$, $r = 1, 2, \ldots, R$, where $R = M + Q$. A graphical depiction of the proposed scenario is presented in Figure 1. The failure of any unit will be observed due to one of two competing causes, indexed by $k = 1, 2$. To accommodate time-varying failure behavior, each stress level is partitioned into subintervals, and under the semiparametric framework the cause-specific hazard for cause k in $(a_r, b_r]$ is modeled using a PMHF. This generalizes the commonly used piecewise constant hazard model. We assume the piecewise monotone hazard function for $i-$th stress, $k-$th cause, and the subinterval $(a_r, b_r]$, as:

$$h_k(t) = \alpha_i \lambda_{k,r} t^{\alpha_i - 1}, \quad t \in (a_r, b_r],$$

where $\lambda_{k,r} > 0$ denotes the scale parameter for cause k in the r-th subinterval, and $\alpha_i > 0$ is the shape parameter associated with the stress level $i \in \{1, 2\}$. Thus, a common shape parameter is assumed within each stress level, while the scale parameters are allowed to vary freely across subintervals, providing substantial flexibility in capturing failure behavior.

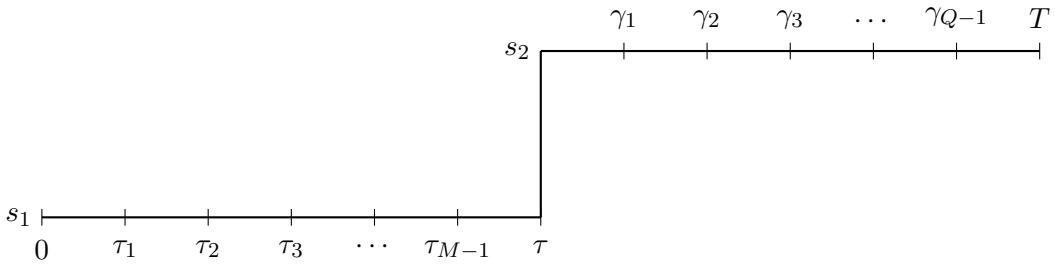

Figure 1: Schematic representation of step-stress model with multiple cut points

To relate the distribution function at two different levels of stress, we have used a flexible failure rate-based model (FRM) (see Kateri and Kamps (2015)[6]). The hazard function of of FRM model

can be expressed as:

$$h(t) = \begin{cases} h_1(t), & 0 < t \leq \tau, \\ h_2(t), & \tau < t < T, \end{cases} \tag{2.1}$$

where $h_1(t)$ and $h_2(t)$ represent the hazard functions associated with the lifetime distributions under stress levels s_1 and s_2, respectively. The FRM formulation provides a natural mechanism to relate the lifetime distributions across stress levels through hazard functions rather than cumulative distributions. This perspective is particularly useful in step-stress experiments, where changes in stress directly affect the instantaneous failure risk rather than the cumulative lifetime distribution alone.

The cumulative hazard function for cause k up to time t is obtained by integrating the corresponding hazard rate over time. Since the hazard is defined piecewise over the subintervals $(a_r, b_r]$, the cumulative hazard is constructed by summing the contributions from each interval. So, the interval-wise cumulative contribution due to cause k can be obtained as

$$H_k(t) = \int_{a_r}^{\min(t,b_r)} \alpha_i \lambda_{k,r} u^{\alpha_i - 1}\, du = \lambda_{k,r} \left\{ \min(t, b_r)^{\alpha_i} - a_r^{\alpha_i} \right\}.$$

Depending on the position of t, three situations arise: before the interval begins, within the interval, and after the interval ends. Accordingly, the cumulative hazard function for cause k can be written as

$$H_k(t) = \sum_{r=1}^{R} \lambda_{k,r} B_r(t; \alpha_i),$$

where the function $B_r(t; \alpha_i)$ represents the accumulated exposure within the rth interval and is defined as

$$B_r(t; \alpha_i) = \begin{cases} 0, & t \leq a_r, \\ t^{\alpha_i} - a_r^{\alpha_i}, & a_r < t \leq b_r, \\ b_r^{\alpha_i} - a_r^{\alpha_i}, & t > b_r. \end{cases} \tag{2.2}$$

When two competing causes of failure are present, the overall cumulative hazard function is obtained as:

$$H(t) = \sum_{k=1}^{2} H_k(t) = \sum_{r=1}^{R} \left(\sum_{k=1}^{2} \lambda_{k,r} \right) B_r(t; \alpha_i).$$

Accordingly, the survival function of a test unit is defined as $S(t) = \exp\{-H(t)\}$, and the cause-specific density function is given by $f_k(t) = h_k(t)S(t)$.

Under the competing risks framework, the observed data consist of both the failure time and the associated cause of failure. Let (t_ℓ, δ_ℓ), $\ell = 1, 2, \ldots, n$, denote the observed data, where t_ℓ represents either the failure time or censoring time for the ℓth unit. The indicator variable $\delta_\ell \in \{0, 1, 2\}$ indicates the failure status, with $\delta_\ell = 0$ corresponding to censored unit at time T, and $\delta_\ell = k$ indicating failure due to cause k for $k = 1, 2$. Under this formulation, the proposed model provides a flexible semiparametric framework capable of capturing complex time-dependent failure patterns induced by step-stress ALT and competing risks.

3 Maximum Likelihood Estimation

In this section, we have discussed the MLEs of model parameters based on the observed data t_ℓ with associated cause of failure δ_ℓ. The likelihood contribution of the ℓth unit depends on the cause of failure

δ_ℓ, and it can be written as

$$L_\ell(\theta) = \begin{cases} \alpha_i \lambda_{1,r}\, t_\ell^{\alpha_i - 1} \exp\{-H(t_\ell)\}\,, & \text{if } \delta_\ell = 1, \\ \alpha_i \lambda_{2,r}\, t_\ell^{\alpha_i - 1} \exp\{-H(t_\ell)\}\,, & \text{if } \delta_\ell = 2, \\ \exp\{-H(t_\ell)\}\,, & \text{if } \delta_\ell = 0, \end{cases} \tag{3.3}$$

where $\theta = (\lambda_{k,r}, \alpha_i)$. The log-likelihood function without additive constant can be written as

$$\log L(\theta) = \sum_{k=1}^{2}\sum_{r=1}^{R} N_{k,r} \log \lambda_{k,r} + \sum_{i=1}^{2} N_i \log \alpha_i + \sum_{i=1}^{2}(\alpha_i - 1) \sum_{\ell \in D_i} \log t_\ell - \sum_{k=1}^{2}\sum_{r=1}^{R} \lambda_{k,r} \left(\sum_{\ell=1}^{n} B_r(t_\ell, \alpha_{i(\ell)}) \right). \tag{3.4}$$

Here, $N_{k,r}$ denotes the number of observed failures due to cause k in interval r. N_i denotes the total number of failures that have been observed during the ith level of stress. D_i denotes the set of failure times observed under the ith stress. For each failure ℓ, let $r(\ell) \in \{1, \ldots, R\}$ denote the interval in which failure occurs, and $i(\ell) \in \{1, 2\}$ be the corresponding stress level active at that failure time t_ℓ. The function $B_r(t_\ell, \alpha_{i(\ell)})$ represents the cumulative hazard contribution in interval r up to time t_ℓ under stress level s_i. The expression for $B_r(t, \alpha_i)$ is given in equation (2.2). The partial derivative of the log-likelihood function with respect to model parameters can be expressed as

$$\frac{\partial \log L(\theta)}{\partial \lambda_{k,r}} = \frac{N_{k,r}}{\lambda_{k,r}} - \sum_{\ell=1}^{n} B_r(t_\ell, \alpha_{i(\ell)}), \quad k = 1, 2, \quad r = 1, \ldots, R. \tag{3.5}$$

$$\frac{\partial \log L(\theta)}{\partial \alpha_i} = \frac{N_i}{\alpha_i} + \sum_{\ell \in D_i} \log t_\ell - \sum_{k=1}^{2}\sum_{r=1}^{R} \lambda_{k,r} \left(\sum_{\ell : i(\ell) = i} B_r'(t_\ell, \alpha_{i(\ell)}) \right), \tag{3.6}$$

where the partial derivative of $B_r(t_\ell, \alpha_i)$ with respect to α_i is given by

$$B_r'(t_\ell, \alpha_i) = \frac{\partial B_r(t_\ell, \alpha_i)}{\partial \alpha_i} = \begin{cases} 0, & t_\ell \le a_r, \\ t_\ell^{\alpha_i} \ln t_\ell - a_r^{\alpha_i} \ln a_r, & a_r < t_\ell \le b_r, \\ b_r^{\alpha_i} \ln b_r - a_r^{\alpha_i} \ln a_r, & t_\ell > b_r. \end{cases} \tag{3.7}$$

The estimate of $\lambda_{k,r}$ can be obtained by equating equation (3.5) to zero. Hence,

$$\hat{\lambda}_{k,r} = \frac{N_{k,r}}{\sum_{\ell=1}^{n} B_r(t_\ell, \alpha_{i(\ell)})}.$$

By plugging the value of $\hat{\lambda}_{k,r}$ in equation (3.6) and equating it with zero, the profile log-likelihood function of α_i can be expressed as

$$\frac{\partial \log L(\theta)}{\partial \alpha_i} = \frac{N_i}{\alpha_i} + \sum_{\ell \in D_i} \log t_\ell - \sum_{k=1}^{2}\sum_{r=1}^{R} \frac{N_{k,r}}{\sum_{\ell : i(\ell) = i} B_r(t_\ell, \alpha_{i(\ell)})} \left(\sum_{\ell : i(\ell) = i} B_r'(t_\ell, \alpha_{i(\ell)}) \right). \tag{3.8}$$

Since a closed-form solution for α_i is difficult to obtain, their estimates are derived by solving the associated one-dimensional nonlinear equations using numerical techniques such as the Newton–Raphson or Broyden method.

3.1 Asymptotic Confidence Interval

Due to the complicated nature of the likelihood function, obtaining exact confidence intervals is analytically difficult. Therefore, we employ asymptotic arguments based on large-sample theory to construct approximate confidence intervals. Under standard regularity conditions, the MLE of the model parameter is asymptotically normally distributed. Consequently, the observed Fisher information matrix for $\theta = (\lambda_{k,r}, \alpha_i)$ can be defined as

$$\mathcal{F}(\theta) = \left(-\frac{\partial^2 \log L(t,\theta)}{\partial\theta_u \, \partial\theta_v} \right).$$

Let $\mathcal{F}^{-1}(\hat{\theta}) = (W_{uv})$ denote the inverse of the observed Fisher information matrix obtained at the MLE. Then, an approximate $100(1-\phi)\%$ asymptotic confidence interval (ACI) for the parameter θ_u is obtained as

$$\hat{\theta}_u \pm z_{1-\phi/2}\sqrt{W_{uu}},$$

where $z_{1-\phi/2}$ represents the $(1-\phi/2)$-quantile of the standard normal distribution. The explicit expressions for the elements of the observed Fisher information matrix are provided below.

$$\frac{\partial^2 \log L}{\partial \lambda_{k,r}^2} = -\frac{N_{k,r}}{\lambda_{k,r}^2}, \quad k = 1,2; \quad r = 1,\ldots,R.$$

$$\frac{\partial^2 \log L}{\partial \alpha_1 \partial \alpha_2} = \frac{\partial^2 \log L}{\partial \alpha_2 \partial \alpha_1} = 0, \quad \frac{\partial^2 \log L}{\partial \lambda_{k,r} \partial \lambda_{k',r'}} = 0, \quad (k,r) \neq (k',r'); \quad k = 1,2; \quad r = 1,\ldots,R.$$

$$\frac{\partial^2 \log L}{\partial \alpha_i^2} = -\frac{N_i}{\alpha_i^2} - \sum_{k=1}^{2}\sum_{r=1}^{R} \lambda_{k,r} \frac{\partial^2 B_r}{\partial \alpha_i^2}, \quad i = 1,2; \quad k = 1,2; \quad r = 1,\ldots R.$$

$$\frac{\partial^2 \log L}{\partial \lambda_{k,r} \partial \alpha_i} = \frac{\partial^2 \log L}{\partial \alpha_i \partial \lambda_{k,r}} = -\sum_{k=1}^{2}\sum_{r=1}^{R} \frac{\partial B_r}{\partial \alpha_i}, \quad i = 1,2; \quad k = 1,2; \quad r = 1,\ldots,R.$$

4 Bayesian Estimation

In this section, we discussed Bayesian estimation of the model parameters, along with both symmetric and highest posterior density (HPD) credible intervals. The analysis is conducted primarily under the squared-error loss function; however, the methodology can be readily extended to accommodate alternative loss functions. We adopt a Gamma distribution with hyperparameters a_i and b_i for the parameters α_i for $i = 1, 2$, whose density function is given by

$$\pi_0(\alpha_i \mid a_i, b_i) \propto e^{-a_i\alpha_i} \alpha_i^{b_i - 1}, \qquad a_i > 0, \; b_i > 0.$$

Further, the scale parameters $(\lambda_{1,r}, \lambda_{2,r})$ for for any given interval $r = 1,\ldots,R$ has been assumed a Gamma–Dirichlet prior. The detailed formulation of the Gamma–Dirichlet prior can be found in Pena and Gupta (1990)[21]. This choice of prior induces dependence between the scale parameters corresponding to each interval. Additionally, when α_i is known, this prior family becomes the conjugate family of priors. The joint prior density of $(\lambda_{1,r}, \lambda_{2,r})$ with hyperparameters $c_r > 0$, $d_r > 0$, $e_r > 0$, and $f_r > 0$ can be expressed as

$$\pi_r(\lambda_{1,r}, \lambda_{2,r} \mid c_r, d_r, e_r, f_r) \propto (\lambda_{1,r} + \lambda_{2,r})^{c_r - e_r - f_r} e^{-d_r(\lambda_{1,r}+\lambda_{2,r})} (\lambda_{1,r})^{e_r - 1} (\lambda_{2,r})^{f_r - 1}.$$

This will be denoted as $\mathrm{GD}(c_r, d_r, e_r, f_r)$. The Gamma–Dirichlet prior adopted for the scale parameters is flexible in modeling failure behaviour across intervals. It allows the total failure rate $(\lambda_{1,r} + \lambda_{2,r})$ and the relative contribution of each cause to be modeled separately. The hyperparameters (c_r, d_r, e_r, f_r)

enable both little and strong informative prior specifications. Moreover, this prior naturally allows dependence between $\lambda_{1,r}$ and $\lambda_{2,r}$, which is realistic in competing-risk and step-stress models, while prior independence is obtained as a special case when $c_r = e_r + f_r$. For a more detailed discussion on this prior one may refer to Pena and Gupta (1990)[21] and Kundu and Pradhan (2011)[22]. We have also assumed that the prior distribution of α_i and $(\lambda_{1,r}, \lambda_{2,r})$ are independent. So, the joint prior distribution can be written as

$$\tilde{\pi}(\lambda_{1,r}, \lambda_{2,r}, \alpha_i) \propto e^{-a_i\alpha_i}\alpha_i^{b_i-1}(\lambda_{1,r}+\lambda_{2,r})^{c_r-e_r-f_r}e^{-d_r(\lambda_{1,r}+\lambda_{2,r})}(\lambda_{1,r})^{e_r-1}(\lambda_{2,r})^{f_r-1}.$$

In most cases, closed-form expressions for the Bayes estimators under the squared error loss function are not available. However, as noted by Kundu and Pradhan (2011)[22], sampling from the joint posterior distribution can be carried out with relative ease. Motivated by this observation, we employ the Gibbs sampling algorithm to obtain the Bayes estimators and the corresponding credible intervals. The joint posterior distribution of the model parameters can therefore be expressed as

$$\Pi(\alpha_i, \lambda_{1,r}, \lambda_{2,r} \mid t) \propto \prod_{i=1}^{2}\prod_{r=1}^{R}\Pi_1(\alpha_i)\Pi_2(\lambda_{1,r}, \lambda_{2,r} \mid \alpha_i), \quad r = 1, \ldots, R; \quad i = 1, 2,$$

where

$$\Pi_1(\alpha_i) \propto e^{-a_i\alpha_i}\alpha_i^{N_i+b_i-1}\left(\prod_{\ell=1}^{N_i} t_\ell\right)^{\alpha_i-1}\left(d_r + \sum_{r=1}^{R} B_r(\alpha_i)\right)^{-(c_r+N_{1,r}+N_{2,r})},$$

$$\Pi_2(\lambda_{1,r}, \lambda_{2,r} \mid \alpha_i) \propto (\lambda_{1,r}+\lambda_{2,r})^{(c_r+N_{1,r}+N_{2,r})-(e_r+N_{1,r})-(f_r+N_{2,r})}(\lambda_{1,r})^{e_r+N_{1,r}-1}(\lambda_{2,r})^{f_r+N_{2,r}-1}$$
$$\times \exp\left\{-\left(d_r + \sum_{r=1}^{R} B_r(\alpha_i)\right)(\lambda_{1,r}+\lambda_{2,r})\right\},$$

$$\Pi_2(\lambda_{1,r}, \lambda_{2,r} \mid \alpha_i) \sim GD\left((c_r+N_{1,r}+N_{2,r}), (d_r + \sum_{r=1}^{R} B_r(\alpha_i)), (e_r+N_{1,r}), (f_r+N_{2,r})\right).$$

The generation of posterior samples from the Gamma-Dirichlet distribution $\Pi_2(\lambda_{1,r}, \lambda_{2,r})$ is straightforward, and it has been discussed in detail by Kundu and Pradhan (2011)[22]. We propose the following Algorithm 1 to compute Bayesian estimates of the model parameters and construct the associated credible intervals.

Algorithm 1 Procedure for Bayesian estimation

1. Generate α_i independently from $\Pi_1(\alpha_i)$ ratio of uniform method proposed by Kinderman and Monahan (1977)[23]. We have mentioned the procedure in Algorithm 2.
2. For given α_i, generate $(\lambda_{1,r}, \lambda_{2,r})$ from $\text{GD}\Big((c_r + N_{1,r} + N_{2,r}), (d_r + \sum_{r=1}^{R} B_r(\alpha_i)), (e_r + N_{1,r}), (f_r + N_{2,r})\Big)$.
3. Repeat Steps 1 and 2 for M iterations to obtain the posterior samples $(\alpha_i^k, \lambda_{1,r}^k, \lambda_{2,r}^k)$, $k = 1, \ldots, M$.
4. Under the squared error loss function, the Bayes estimators are given by the posterior means:
$$\hat{\alpha}_i = \frac{1}{M}\sum_{k=1}^{M} \alpha_i^k, \qquad \hat{\lambda}_{1,r} = \frac{1}{M}\sum_{k=1}^{M} \lambda_{1,r}^k, \qquad \hat{\lambda}_{2,r} = \frac{1}{M}\sum_{k=1}^{M} \lambda_{2,r}^k.$$
5. To construct a $100(1-\phi)\%$ symmetric credible interval for α_i, first arrange the samples $\alpha_i^1, \ldots, \alpha_i^M$ in ascending order: $\alpha_i^1 < \alpha_i^2 < \cdots < \alpha_i^M$. Then the symmetric credible interval is given by
$$\left(\alpha_i^{\left(\left\lfloor \frac{\phi M}{2} \right\rfloor\right)}, \alpha_i^{\left(\left\lfloor (1-\frac{\phi}{2})M \right\rfloor\right)}\right).$$
6. To obtain the $100(1-\phi)\%$ HPD credible interval, consider the intervals
$$\left(\alpha_i^{(j)}, \alpha_i^{(j+\lfloor (1-\phi)M \rfloor)}\right), \quad j = 1, \ldots, \lfloor \phi M \rfloor.$$
The HPD credible interval is chosen as $\left(\alpha_i^{(j^*)}, \alpha_i^{(j^*+\lfloor (1-\phi)M \rfloor)}\right)$, where j^* minimizes the interval length.

Algorithm 2 Procedure for ratio of uniform method

1. Generate two independent random variables V_1 and V_2 from the Uniform$(0, 1)$ distribution.
2. For $i = 1, 2$, check whether $V_1 < \sqrt{\frac{\Pi_1(V_2/V_1)}{\int_0^\infty \Pi_1(\alpha_i)\, d\alpha_i}}$ holds or not.
3. For $i = 1, 2$, if $V_1 < \sqrt{\frac{\Pi_1(V_2/V_1)}{\int_0^\infty \Pi_1(\alpha_i)\, d\alpha_i}}$, then $\alpha_i^* = V_2/V_1$ has the density function $\frac{\Pi_1(\alpha_i)}{\int_0^\infty \Pi_1(\alpha_i)\, d\alpha_i}$, otherwise repeat Steps 1–2.

5 Simulation Study

An extensive Monte Carlo simulation study has been conducted to investigate the proposed framework under both classical and Bayesian setups. For illustrative purposes, we have assumed one cut point at each level of stress. Accordingly, the model parameters under stress level s_1 are $\alpha_1, \lambda_{1,1}, \lambda_{2,1}, \lambda_{1,2}, \lambda_{2,2}$, whereas under stress level s_2 the parameters are $\alpha_2, \lambda_{1,3}, \lambda_{2,3}, \lambda_{1,4}, \lambda_{2,4}$. Although only one cut point per

stress level has been assumed in this section, but the proposed framework can be extended similarly to incorporate multiple cut points without altering the proposed methodology. For the simulation purpose, we have taken the true values of the parameters are $\alpha_1 = 1.2, \lambda_{1,1} = 0.3, \lambda_{2,1} = 0.6, \lambda_{1,2} = 0.9, \lambda_{2,2} = 1.2$, and $\alpha_2 = 2.2, \lambda_{1,3} = 1.5, \lambda_{2,3} = 1.8, \lambda_{1,4} = 2.1, \lambda_{2,4} = 2.4$. Further, the stress changing time is set to $\tau = 0.45$ and the termination time to $T = 0.9$. The first cut point under the stress level s_1 is taken as $\tau_1 = 0.3$, while the second cut point under the stress level s_2 is fixed at $\gamma_1 = 0.6$. The experiments are carried out for several sample sizes: $n = 60, 80, 100, 120, 200, 260, 300$. The data sets are generated using the procedure described in Algorithm (3). In both setups, we have computed the results based on 2000 replications. The average estimates (AEs) and mean squared errors (MSEs) of MLEs are obtained and they are reported in Table 1, while the average interval lengths along with coverage percentages (CPs) of the 95% ACIs are noted in Table 2. We have obtained Bayesian estimates (BEs) and associated credible intervals for the model parameters under the squared-error loss function. For the Bayes estimation, we have considered almost noninformative priors, which have also been suggested by Congdon (2014)[24]. The hyperparameters are taken as: $a_1 = b_1 = a_2 = b_2 = c_1 = d_1 = c_2 = d_2 = c_3 = d_3 = c_4 = d_4 = 0.001$, and $e_1 = f_1 = e_2 = f_2 = e_3 = f_3 = e_4 = f_4 = 1$. Table 3 presents the average estimates along with MSEs of the BEs for the model parameters. Both 95% symmetric and HPD credible intervals are constructed along with CPs, and results have been presented in Tables 4 and 5.

The simulation results demonstrate that the proposed MLE and Bayesian procedures yield very similar performance in terms of MSEs across all sample sizes considered. In both frameworks, the MSEs and interval lengths decrease as the sample size increases, providing strong evidence for the consistency of the proposed estimators. Moreover, the CPs are close to their nominal levels, indicating that both ACIs and credible intervals are reliable. It is further observed that the average length of HPD intervals is typically shorter than the corresponding symmetric credible intervals while maintaining comparable coverage probabilities, reflecting the improved efficiency of HPD-based uncertainty quantification. Overall, the simulation study confirms the effectiveness and robustness of the proposed inferential procedures for semi–parametric step–stress competing risks models.

Algorithm 3 Data Generation Procedure for semiparametric Step Stress ALT

1. For given n, τ and T, generate n independent random variables $u_1, u_2, \ldots, u_n \sim U(0,1)$, and sort them in ascending order.

2. Let $0 < \tau_1 < \tau_2 < \cdots < \tau_M = \tau$ be the cut points under stress level s_1, and $\tau < \gamma_1 < \gamma_2 < \cdots < \gamma_Q = T$ be the cut points under stress level s_2.

3. For the first interval $(0, \tau_1]$, compute $z_1 = F_1(\tau_1)$, where $F_1(\cdot)$ denotes the cumulative distribution function up to time τ_1. For each unit ℓ such that random variable $u_\ell \leq z_1$, set $t_\ell = F_1^{-1}(u_\ell)$. To assign the cause of failure, generate $w_\ell \sim U(0,1)$. If $w_\ell < \frac{\lambda_{1,1}}{\lambda_{1,1}+\lambda_{2,1}}$, then $\delta_\ell = 1$; otherwise $\delta_\ell = 2$.

4. All surviving units satisfying $u_\ell > z_1$ are transferred to the next interval $(\tau_1, \tau_2]$ under stress level s_1.

5. For the interval $(\tau_1, \tau_2]$, compute $z_2 = F_2(\tau_2)$, where $F_2(\cdot)$ denotes the cumulative distribution function up to time τ_2. For each unit ℓ such that $u_\ell \leq z_2$, set $t_\ell = F_2^{-1}(u_\ell)$, and similarly to assign the cause of failure generate $w_\ell \sim U(0,1)$. If $w_\ell < \frac{\lambda_{2,2}}{\lambda_{1,2}+\lambda_{2,2}}$, then $\delta_\ell = 1$; otherwise $\delta_\ell = 2$.

6. Repeat Steps 3–5 sequentially for all $R = M + Q$ intervals across both stress levels.

7. Any unit for which $u_\ell > F_R(T)$ is treated as right–censored at time T.

Table 1: Average estimate and MSE (in bracket) of the model parameters based on MLE for several values of n

n	α_1	$\lambda_{1,1}$	$\lambda_{2,1}$	$\lambda_{1,2}$	$\lambda_{2,2}$	α_2	$\lambda_{1,3}$	$\lambda_{2,3}$	$\lambda_{1,4}$	$\lambda_{2,4}$
60	1.3062	0.4257	0.8081	0.9795	1.3116	2.6453	1.9760	2.3869	2.4200	2.7727
	(0.1845)	(2.6443)	(1.8529)	(0.2311)	(0.3456)	(1.5340)	(1.2982)	(1.7947)	(1.1322)	(1.4156)
80	1.2818	0.3676	0.7301	0.9583	1.2877	2.5366	1.9240	2.2798	2.4184	2.7708
	(0.1261)	(0.0971)	(0.2685)	(0.1473)	(0.2254)	(1.3666)	(1.0126)	(1.2687)	(0.9280)	(1.1872)
100	1.2698	0.3521	0.7004	0.9420	1.2557	2.4970	1.8593	2.2482	2.3627	2.7168
	(0.0938)	(0.0476)	(0.1532)	(0.1088)	(0.1523)	(1.2449)	(0.8196)	(1.1044)	(0.7402)	(0.9401)
160	1.2335	0.3249	0.6502	0.9294	1.2338	2.4059	1.7669	2.1280	2.3156	2.6578
	(0.0503)	(0.0209)	(0.0617)	(0.0622)	(0.0827)	(0.9446)	(0.4802)	(0.6301)	(0.5088)	(0.6493)
200	1.2356	0.3231	0.6466	0.9220	1.2267	2.3329	1.7159	2.0678	2.3104	2.6407
	(0.0401)	(0.0160)	(0.0471)	(0.0468)	(0.0657)	(0.8071)	(0.3352)	(0.4558)	(0.4486)	(0.5718)
260	1.2264	0.3171	0.6357	0.9155	1.2234	2.2971	1.6722	2.0057	2.2898	2.6031
	(0.0298)	(0.0116)	(0.0331)	(0.0365)	(0.0485)	(0.6694)	(0.2515)	(0.3187)	(0.3562)	(0.4124)
300	1.2193	0.3137	0.6295	0.9134	1.2204	2.2674	1.6480	1.9774	2.2676	2.5937
	(0.0263)	(0.0099)	(0.0291)	(0.0312)	(0.0424)	(0.5959)	(0.2025)	(0.2596)	(0.2998)	(0.3866)

Table 2: Average length and CP of 95% ACI for the model parameters based on MLE for several values of n

n	α_1	$\lambda_{1,1}$	$\lambda_{2,1}$	$\lambda_{1,2}$	$\lambda_{2,2}$	α_2	$\lambda_{1,3}$	$\lambda_{2,3}$	$\lambda_{1,4}$	$\lambda_{2,4}$
60	1.4852	1.1174	1.8910	1.6837	2.0197	5.9746	4.7634	5.6398	5.0752	5.7088
	95.46	90.58	91.66	92.88	93.60	100	90.58	97.38	95.38	96.12
80	1.2618	0.8173	1.4673	1.4233	1.6871	5.2789	4.1678	4.8209	4.6083	5.2102
	95.36	90.56	92.44	93.88	93.82	99.98	90.56	97.58	95.94	96.12
100	1.1132	0.7157	1.2670	1.2467	1.4625	4.8206	3.6787	4.3398	4.0565	4.5567
	95.26	92.14	93.28	93.70	94.08	99.42	92.14	97.16	95.64	96.26
160	0.8506	0.5322	0.9115	0.9593	1.1157	3.9788	2.7697	3.2242	3.1181	3.4959
	95.26	92.48	93.74	94.16	95.12	97.36	92.48	98.00	96.14	96.18
200	0.7604	0.4734	0.8064	0.8518	0.9908	3.6079	2.3502	2.7319	2.8231	3.1496
	95.52	93.14	94.46	94.6	95.12	97.04	93.14	97.80	96.16	96.42
260	0.6605	0.4051	0.6878	0.7413	0.8629	3.2191	1.9541	2.2539	2.3899	2.636
	95.20	93.70	94.70	94.48	95.12	96.80	93.70	97.52	96.36	97.10
300	0.6110	0.3716	0.6307	0.6876	0.8001	3.0176	1.7678	2.0351	2.1795	2.4326
	94.52	93.54	94.44	94.24	94.90	95.82	93.54	97.62	96.62	96.80

Table 3: Average estimate and MSE (in bracket) of the model parameters based on Bayesian estimation for several values of n

n	α_1	$\lambda_{1,1}$	$\lambda_{2,1}$	$\lambda_{1,2}$	$\lambda_{2,2}$	α_2	$\lambda_{1,3}$	$\lambda_{2,3}$	$\lambda_{1,4}$	$\lambda_{2,4}$
60	1.2786	0.5242	0.9414	1.0727	1.3681	2.0458	1.9386	2.2824	2.8555	3.1927
	(0.1417)	(0.4893)	(1.2404)	(0.2675)	(0.3454)	(0.3826)	(0.7877)	(0.9873)	(1.5229)	(1.7494)
80	1.2502	0.4306	0.8048	1.0154	1.3168	2.0185	1.8954	2.2181	2.8057	3.1556
	(0.1011)	(0.1785)	(0.5116)	(0.1527)	(0.2156)	(0.3819)	(0.5973)	(0.7136)	(1.2402)	(1.4376)
100	1.2373	0.3951	0.7365	0.9916	1.2961	1.9802	1.8415	2.1889	2.7536	3.127
	(0.0758)	(0.0681)	(0.2137)	(0.1136)	(0.1557)	(0.4037)	(0.4562)	(0.5855)	(1.0328)	(1.2604)
160	1.2199	0.3498	0.6687	0.9548	1.2502	1.9414	1.7785	2.1123	2.7017	3.0768
	(0.044)	(0.025)	(0.0688)	(0.0625)	(0.0879)	(0.4255)	(0.3089)	(0.3839)	(0.7951)	(0.9485)
200	1.2132	0.3386	0.6554	0.9442	1.2386	1.9095	1.7409	2.0708	2.6727	3.0357
	(0.0348)	(0.0186)	(0.0512)	(0.0474)	(0.0660)	(0.4369)	(0.2476)	(0.3028)	(0.6852)	(0.8083)
260	1.2109	0.3315	0.6397	0.9365	1.236	1.9304	1.7223	2.0504	2.6155	2.9882
	(0.0278)	(0.0129)	(0.0357)	(0.0374)	(0.0505)	(0.4326)	(0.2010)	(0.2581)	(0.5494)	(0.7012)
300	1.2101	0.3243	0.6353	0.9314	1.2268	1.9113	1.6951	2.0167	2.5986	2.9558
	(0.0232)	(0.0101)	(0.0293)	(0.0307)	(0.0419)	(0.4132)	(0.1607)	(0.2103)	(0.5176)	(0.6257)

Table 4: Average length and CP of 95% symmetric credible intervals for the model parameters based on Bayesian estimation for several values of n

n	α_1	$\lambda_{1,1}$	$\lambda_{2,1}$	$\lambda_{1,2}$	$\lambda_{2,2}$	α_2	$\lambda_{1,3}$	$\lambda_{2,3}$	$\lambda_{1,4}$	$\lambda_{2,4}$
60	1.5808	2.0236	3.3947	1.9599	2.3007	4.1358	4.0268	4.5703	4.8185	5.2254
	96.6	96.58	95.92	95.28	97.26	99.72	96.7	96.62	95.98	95.64
80	1.3485	1.31	2.2367	1.5434	1.823	3.9787	3.5919	4.0671	4.3535	4.754
	96.7	96.88	95.88	95.4	97.38	99.42	96.48	97.16	95.18	95.2
100	1.2023	1.0017	1.6957	1.3199	1.5537	3.804	3.235	3.7049	4.0182	4.4282
	96.8	96.54	95.62	95.5	97.48	99.12	97.16	97.22	94.92	94.96
160	0.9584	0.665	1.13	0.9901	1.1563	3.4619	2.6316	3.0184	3.451	3.8275
	96.96	96.88	95.36	95	97.84	98.14	97.04	97.44	93.86	94.24
200	0.8594	0.5693	0.9737	0.8734	1.0173	3.2582	2.3299	2.6715	3.2141	3.5653
	96.92	96.82	95.3	95.22	97.86	97.24	97.3	97.68	94.08	93.92
260	0.7631	0.4868	0.8293	0.7603	0.8865	3.0832	2.079	2.3907	2.8917	3.2273
	97.12	97.14	95.36	95.26	97.4	96.28	97.58	97.52	94.26	93.48
300	0.7159	0.4435	0.7646	0.7035	0.8186	2.954	1.8885	2.1738	2.7532	3.0655
	97.28	97.68	96.06	95.48	97.88	95.96	97.3	97.34	93.28	93.94

Table 5: Average length and CP of 95% HPD credible intervals for the model parameters based on Bayesian estimation for several values of n

n	α_1	$\lambda_{1,1}$	$\lambda_{2,1}$	$\lambda_{1,2}$	$\lambda_{2,2}$	α_2	$\lambda_{1,3}$	$\lambda_{2,3}$	$\lambda_{1,4}$	$\lambda_{2,4}$
60	1.5488	1.5335	2.6145	1.7835	2.1052	3.7559	3.5168	3.998	4.4549	4.8423
	95.62	94.8	95.76	95.06	96.52	98.38	97.56	97.7	98.34	98.18
80	1.3277	1.0682	1.8522	1.4511	1.7213	3.6262	3.1638	3.586	4.046	4.4231
	95.58	95.74	95.18	95.44	97.08	97.66	97.9	98.18	98.18	97.96
100	1.1872	0.8568	1.4703	1.2627	1.4923	3.4805	2.8751	3.293	3.7452	4.1324
	95.9	95.68	94.7	95.34	97.12	96.46	98.44	98.46	97.82	98.22
160	0.9504	0.6036	1.0367	0.966	1.131	3.221	2.3806	2.7285	3.226	3.5767
	95.82	96.02	95.36	94.94	97.34	94.3	98.6	98.68	97.54	97.84
200	0.8533	0.5262	0.9086	0.8566	1.0001	3.0579	2.1311	2.442	3.0048	3.3314
	96.22	96.5	95.56	95.32	97.72	93.22	98.48	99	97.58	97.82
260	0.7587	0.4574	0.785	0.7488	0.8748	2.937	1.9208	2.2059	2.6971	3.0074
	96.84	96.48	95.16	95.36	97.32	91.9	99.1	98.94	97.64	97.3
300	0.7121	0.4199	0.7287	0.6944	0.8092	2.8307	1.7574	2.0193	2.5652	2.8511
	96.74	97.06	96.06	95.56	97.84	91.46	98.82	98.84	97.22	97.58

6 Data Analysis

In this section, a real dataset is analyzed to illustrate the applicability and effectiveness of the proposed semiparametric step-stress model under competing risks. The dataset originates from a study of individuals infected with the human immunodeficiency virus (HIV) and has been widely utilized in the survival analysis and reliability literature. According to the data collection, the study includes 329 men who had sex with men (MSM) who were diagnosed with HIV and were followed over several years until disease progression or death due to AIDS-related causes. These individuals had been diagnosed with HIV for nearly 20 years, providing a long follow-up period for studying disease progression. Despite

changes in sexual risk behavior within the homosexual population, HIV has continued to spread widely among MSM. According to estimates from the United States Centers for Disease Control and Prevention (CDC), MSM accounted for approximately 40% of newly reported HIV cases in 1996 and 54% of all reported adult AIDS cases in the United States between 1990 and 1996. In addition, about 7% of cumulative AIDS cases and 5% of new cases in 1996 were attributed to individuals with dual exposure, namely MSM and injection drug use. The data were collected during the period when antiretroviral combination therapy became available, making the dataset particularly relevant for understanding HIV disease progression under evolving treatment conditions. A detailed clinical and epidemiological description of the data can be found in Dukers et al. (2000)[25] and Xiridou et al. (2003)[26]. This dataset has also been used as an illustrative example for comparing different competing risk analysis methods, as reported in Putter et al. (2007)[27], Geskus et al. (2016)[28], and Alotaibi et al. (2023)[29]. In these studies, two competing risk factors are observed in the data. The first risk factor corresponds to the diagnosis of AIDS, which represents the most severe stage of HIV infection. The second risk factor is the appearance of the syncytium-inducing (SI) HIV phenotype, which is associated with rapid immune system deterioration and a poorer prognosis. For some patients, neither event was observed during the follow-up period, either because they did not experience disease progression or because they died from other causes. Such observations are therefore treated as censored. In the analysis, only the first occurring event is observed for each patient. If AIDS occurs before the SI phenotype appears, the SI event cannot be observed, and vice versa. Therefore, the two events are treated as competing risks. This structure allows the data to be naturally modeled using competing risk methodologies.

For inference purposes, we have taken only those individuals with complete information on failure time and cause of failure. After excluding observations with incomplete or ambiguous event information, the sample size is reduced to 222 patients. Among these, 217 events are observed before the end of the study, while the remaining observations are right-censored. All analyses in this study are based on these 222 individuals. The failure data sets due to each cause are presented in Table 6, which has been taken from Alotaibi et al. (2024)[29]. In the present analysis, time itself is treated as the stress factor. This modeling choice reflects the fact that, as time since HIV infection progresses, the physiological burden on the immune system increases, leading to a higher risk of disease progression and failure events. Instead of assuming a constant risk over time, a step-stress framework is adopted to capture abrupt changes in disease dynamics at clinically meaningful time points. For modeling under the semiparametric set-up, we have considered one cut point at both stress levels. Specifically, the stress-changing times are fixed at $\tau = 6$ years, and the cut point at step 1 is $\tau_1 = 3$ years. Furthermore, the experiment is terminated at the stopping time $T = 12$ years, and another cut point at step 2 is $\gamma_1 = 9$ years. Accordingly, the total observation period is divided into four time intervals $(0, \tau_1], (\tau_1, \tau], (\tau, \gamma], (\gamma, T]$. We have also presented the observed failure times for each interval, along with the associated cause in Table 7.

To evaluate the goodness of fit of the proposed models, the Kolmogorov–Smirnov (KS) distance between the empirical and fitted CDFs was computed, along with the corresponding p-values. The obtained KS statistics and p-values are 0.023 and 0.9901, respectively, indicating that the fitted models provide an adequate representation of the data. We compare the proposed model with the PCHF model under two scenarios: with cut points and without cut points. In addition, we compare the proposed model with the piecewise Weibull hazard model under the assumption of no cut points. The comparisons are presented using both graphical illustrations and goodness-of-fit measures such as the KS distance and Akaike Information Criterion (AIC). In Figure 2, the empirical and fitted CDFs based on the MLEs are plotted for the PCHF model under both scenarios. It can be observed that the fit improves when cut points are incorporated. Similarly, Figure 3 presents the empirical and fitted CDFs for the PMHF model with and without cut points. Again, the model with cut points provides a better fit to the data. A comprehensive comparison of all models is summarized in Table 8 using the KS distance and AIC values. From the table, it is clear that the minimum KS distance and AIC

are obtained for the proposed PMHF model with two cut points, indicating that it provides the best fit among the competing models. These results demonstrate that the proposed model offers greater flexibility than the existing models. The PCHF model can be obtained as a special case of the proposed model when the shape parameter equals one. Furthermore, when no cut points are considered, the proposed framework reduces to the standard step-stress competing risk model based on the PMHF. The analysis further illustrates the practical benefit of the proposed PMHF model, which captures changing risk patterns more effectively than PCHF alternatives.

Further, the profile log-likelihood functions for α_1 and α_2 are plotted in Figure 4. Both profiles are unimodal and attain a unique maximum, indicated by the dotted vertical lines. In addition, Table 9 reports the average parameter estimates together with the corresponding lower and upper bounds of the 95% ACIs, symmetric credible intervals, and HPD credible intervals, obtained using both maximum likelihood and Bayesian methods for the dataset.

Table 6: Failure time observations corresponding to two competing causes for the AIDS dataset

First cause	Second cause
9.106, 2.234, 3.819, 6.801, 3.953, 10.078, 5.018, 9.895, 10.196, 8.755, 8.191, 2.705, 2.672, 3.724, 5.251, 10.453, 9.694, 5.667, 6.955, 10.903, 10.067, 12.129, 8.638, 5.618, 10.889, 3.513, 2.177, 4.608, 6.054, 11.469, 3.647, 6.224, 11.201, 9.137, 2.533, 6.177, 1.837, 10.303, 4.099, 3.064, 10.530, 9.473, 9.555, 9.733, 1.440, 5.555, 6.733, 7.781, 10.847, 8.066, 5.723, 3.373, 6.045, 3.477, 5.566, 2.155, 2.683, 4.811, 3.707, 4.219, 11.387, 8.986, 7.499, 7.825, 7.349, 3.486, 4.981, 3.242, 4.583, 8.304, 6.579, 6.461, 3.214, 5.582, 3.800, 3.592, 5.678, 6.267, 3.663, 4.219, 2.875, 3.975, 6.866, 4.690, 11.247, 13.361, 6.412, 7.006, 3.535, 8.495, 9.051, 10.647, 6.195, 9.246, 5.013, 7.461, 9.202, 3.315, 5.574, 2.891, 7.302, 8.586, 3.639, 8.358, 3.195, 7.553, 2.283, 9.070, 5.938, 6.042, 6.199, 10.730, 9.068, 10.117	9.878, 8.605, 6.218, 6.820, 1.503, 5.525, 1.889, 5.106, 7.409, 6.018, 6.979, 2.322, 7.904, 7.170, 5.886, 5.082, 9.897, 5.889, 1.593, 2.866, 5.336, 6.943, 0.474, 3.439, 7.751, 0.824, 10.617, 3.880, 3.797, 9.437, 9.566, 5.563, 11.020, 0.703, 4.389, 1.462, 0.137, 9.070, 5.700, 5.730, 12.400, 4.854, 11.696, 3.220, 5.478, 4.523, 3.584, 5.908, 4.966, 2.982, 4.734, 3.039, 5.021, 5.224, 4.334, 3.258, 3.064, 2.513, 6.311, 3.817, 13.936, 7.589, 11.943, 5.374, 4.079, 10.809, 5.982, 10.448, 9.777, 6.516, 4.375, 4.520, 2.053, 2.048, 6.042, 10.467, 12.936, 4.230, 9.733, 3.477, 4.909, 7.721, 9.084, 2.565, 2.814, 6.850, 6.439, 0.884, 4.394, 8.142, 1.205, 1.101, 0.969, 2.798, 3.940, 4.400, 5.454, 5.120, 4.033, 6.511, 1.013, 5.736, 9.440, 7.537, 2.571, 0.112, 5.314, 2.631

Table 7: Observed failure times in each interval due to each cause for the AIDS dataset

Interval	Failures due to cause-1	Failures due to cause-2
$(0, 3]$	1.440, 1.837, 2.155, 2.177, 2.234, 2.283, 2.533, 2.672, 2.683, 2.705, 2.875, 2.891	0.112, 0.137, 0.474, 0.703, 0.824, 0.884, 0.969, 1.013, 1.101, 1.205, 1.462, 1.503, 1.593, 1.889, 2.048, 2.053, 2.322, 2.513, 2.565, 2.571, 2.631, 2.798, 2.814, 2.866, 2.982
$(3, 6]$	3.064, 3.195, 3.214, 3.242, 3.315, 3.373, 3.477, 3.486, 3.513, 3.535, 3.592, 3.639, 3.647, 3.663, 3.707, 3.724, 3.800, 3.819, 3.953, 3.975, 4.099, 4.219, 4.219, 4.583, 4.608, 4.690, 4.811, 4.981, 5.013, 5.018, 5.251, 5.555, 5.566, 5.574, 5.582, 5.618, 5.667, 5.678, 5.723, 5.938	3.039, 3.064, 3.220, 3.258, 3.439, 3.477, 3.584, 3.797, 3.817, 3.880, 3.940, 4.033, 4.079, 4.230, 4.334, 4.375, 4.389, 4.394, 4.400, 4.520, 4.523, 4.734, 4.854, 4.909, 4.966, 5.021, 5.082, 5.106, 5.120, 5.224, 5.314, 5.336, 5.374, 5.454, 5.478, 5.525, 5.563, 5.700, 5.730, 5.736, 5.886, 5.889, 5.908, 5.982
$(6, 9]$	6.042, 6.045, 6.054, 6.177, 6.195, 6.199, 6.224, 6.267, 6.412, 6.461, 6.579, 6.733, 6.801, 6.866, 6.955, 7.006, 7.302, 7.349, 7.461, 7.499, 7.553, 7.781, 7.825, 8.066, 8.191, 8.304, 8.358, 8.495, 8.586, 8.638, 8.755, 8.986	6.018, 6.042, 6.218, 6.311, 6.439, 6.511, 6.516, 6.820, 6.850, 6.943, 6.979, 7.170, 7.409, 7.537, 7.589, 7.721, 7.751, 7.904, 8.142, 8.605
$(9, 12]$	9.051, 9.068, 9.070, 9.106, 9.137, 9.202, 9.246, 9.473, 9.555, 9.694, 9.733, 9.895, 10.067, 10.078, 10.117, 10.196, 10.303, 10.453, 10.530, 10.647, 10.730, 10.847, 10.889, 10.903, 11.201, 11.247, 11.387, 11.469	9.070, 9.084, 9.437, 9.440, 9.566, 9.733, 9.777, 9.878, 9.897, 10.448, 10.467, 10.617, 10.809, 11.020, 11.696, 11.943

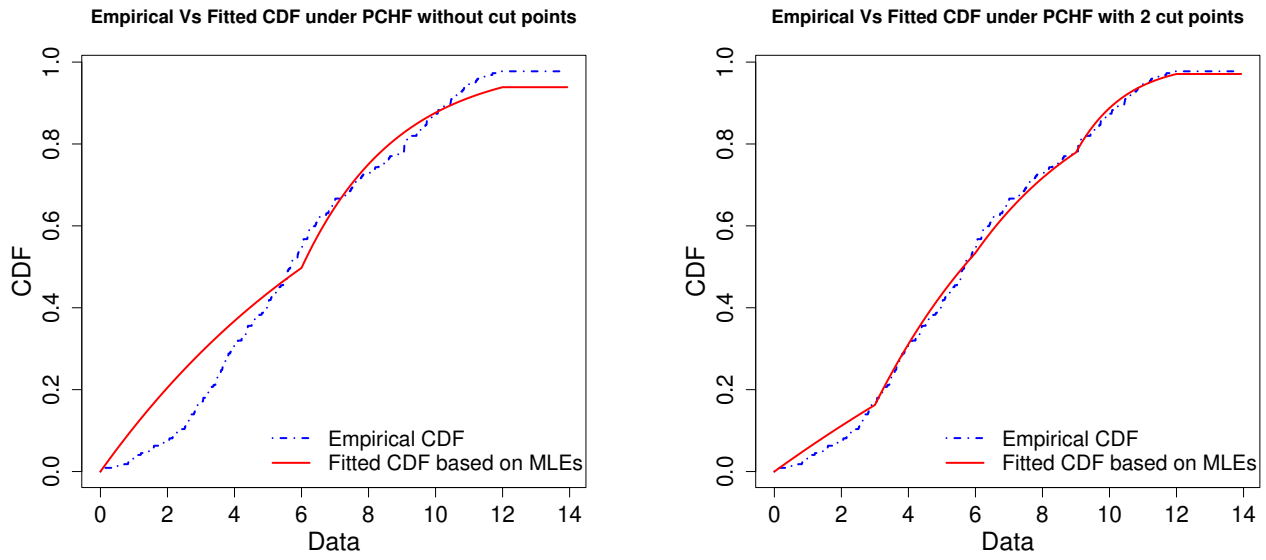

Figure 2: Plot of empirical versus fitted CDFs for the AIDS dataset under PCHF with and without cut points

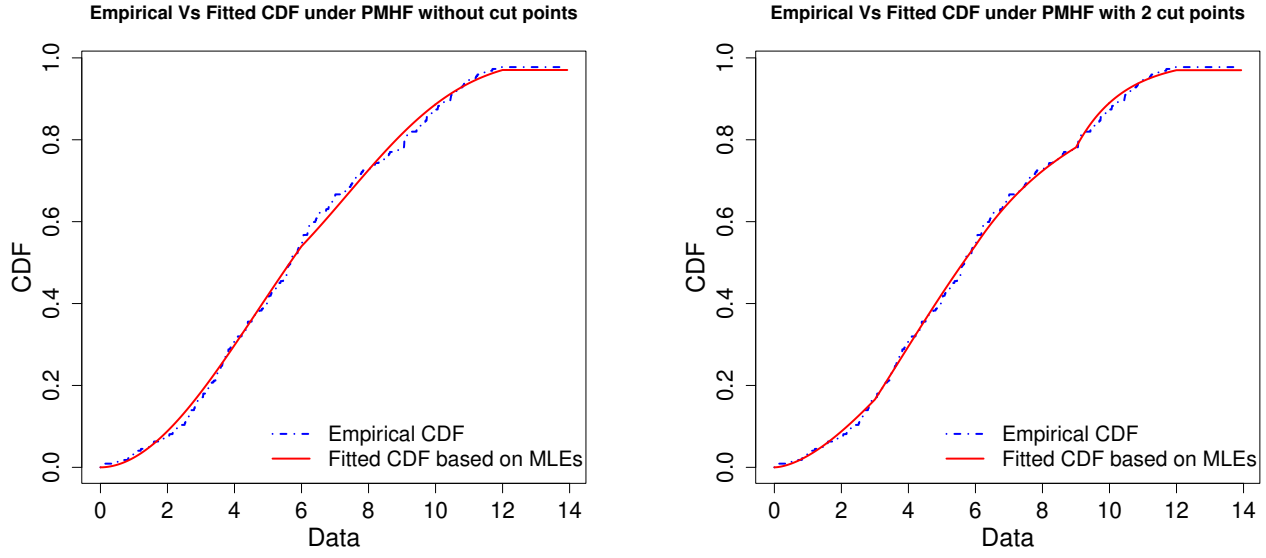

Figure 3: Plot of empirical versus fitted CDFs for the AIDS dataset under PMHF with and without cut points

Table 8: Comparison of PCHF and PMHF models with and without cut points

(M,Q)	PCHF		PMHF	
	KS	AIC	KS	AIC
(1,1)	0.1464	1463.77	0.0392	1401.44
(2,2)	0.0415	1402.52	0.0231	1396.26

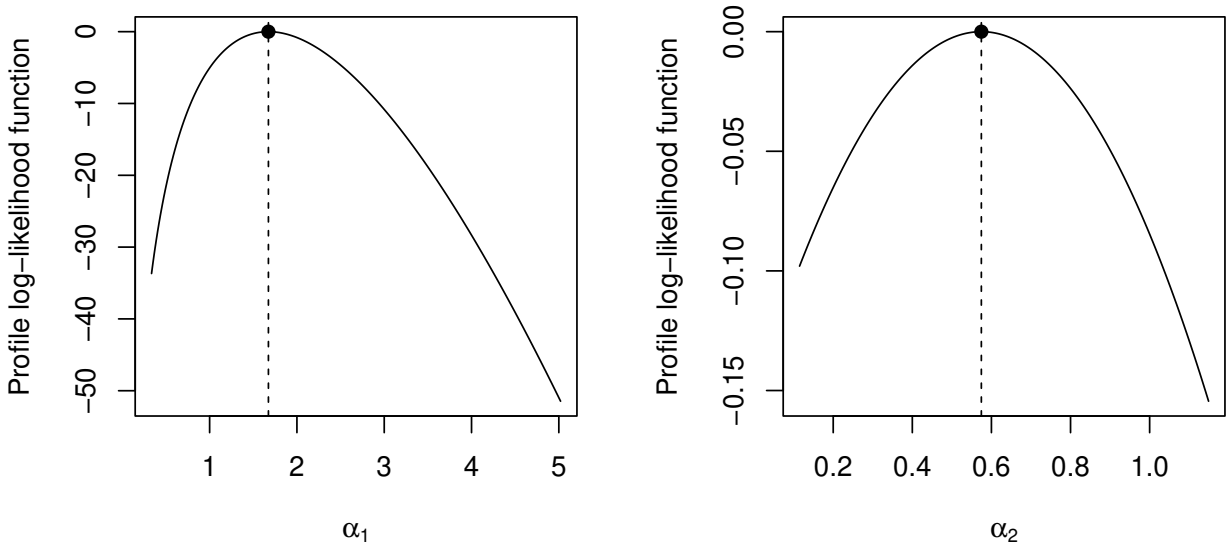

Figure 4: Unimodality of profile log-likelihood of α_1 and α_2 based on the AIDS dataset

Table 9: Average estimates and corresponding confidence intervals for the AIDS dataset

Parameter	MLE estimates	ACI	Bayes estimates	Credible interval	HPD interval
α_1	1.6733	(1.1974,2.1493)	1.5984	(1.2062,2.1203)	(1.1867,2.0808)
$\lambda_{1,1}$	0.0093	(0.0022,0.0165)	0.0108	(0.0043,0.0205)	(0.0035,0.0191)
$\lambda_{2,1}$	0.0195	(0.0069,0.0321)	0.0215	(0.0101,0.0376)	(0.0091,0.0357)
$\lambda_{1,2}$	0.0207	(0,0.0422)	0.0285	(0.0079,0.0625)	(0.0063,0.0573)
$\lambda_{2,2}$	0.0228	(0,0.0463)	0.0311	(0.0088,0.0671)	(0.0072,0.0621)
α_2	0.5745	(0,2.6050)	0.8101	(0.2183,2.1956)	(0.2002,1.9692)
$\lambda_{1,3}$	0.6202	(0,5.3088)	0.8639	(0.0058,3.3425)	(0.0001,2.8923)
$\lambda_{2,3}$	0.3876	(0,3.3199)	0.5484	(0.0037,2.1495)	(0.0001,1.8388)
$\lambda_{1,4}$	1.9884	(0,18.3078)	2.9382	(0.0116,11.9961)	(0.0002,10.3362)
$\lambda_{2,4}$	1.1362	(0,10.4687)	1.7241	(0.0062,7.1565)	(0.0001,6.2105)

6.1 Hypothesis testing for shape parameters

The proposed framework generalizes the PCHF model by allowing the shape parameters to vary across stress levels. In particular, when $\alpha_i = 1$ $(i = 1, 2)$, the hazard rate becomes constant within each subinterval, and it reduces to a PCHF model. It is therefore of interest to test whether such a simplified structure is adequate for the AIDS dataset. We consider the following hypotheses:

$$H_0 : \alpha_1 = \alpha_2 = 1 \qquad \textbf{vs} \qquad H_1 : \alpha_1 \neq \alpha_2 \neq 1$$

The hypotheses are tested using the likelihood ratio test (LRT). Let $\ell(\tilde{\theta})$ and $\ell(\hat{\theta})$ denote the maximized log-likelihood under the null hypothesis and alternate hypothesis respectively. The LRT statistic is given by

$$\Lambda = -2\left[\ell(\tilde{\theta}) - \ell(\hat{\theta})\right].$$

Under the null hypothesis, Λ asymptotically follows a chi-square distribution with degrees of freedom equal to the number of constraints imposed under the null hypothesis. Under H_0 and H_1, the value of $\ell(\tilde{\theta}) = -693.2592$ and $\ell(\hat{\theta}) = -688.1295$ has been obtained. We obtained the value of LRT statistic $\Lambda = 10.2594$ and corresponding p value is 0.0059. Thus, we reject the null hypothesis for 5% level of significance. Hence, it indicate that the PCHF assumption is not adequate for the observed data. Which suggests that the failure risk varies within intervals, and the proposed PMHF model provides a more appropriate representation of the failure behavior.

6.2 Choice of Cut Points

In the earlier sections, the number and locations of the cut points were assumed to be known. However, for a given data set, these are not known. In this section, we will discuss the method to obtain the positions of the cut points from the data. Let τ denote the maximum observed lifetime on s_1. The positions of the cut points $(\tau_1, \ldots \tau_{M-1})$ in the interval $(0, \tau]$ are modeled as the arrival times of a non-homogeneous Poisson process (NHPP) $\{N_1(t); t \geq 0\}$ with intensity function $u_1(t) = \beta_1 t^{\beta_1 - 1}, \quad \beta_1 > 0$. The arrival times of the NHPP are not observed and are therefore treated as missing values. For a fixed number of cut points $M-1$ in $(0, \tau]$, the likelihood function of the lifetime data is expressed as a function of the model parameters $\lambda_{k,r}, \alpha_1$ and the NHPP parameter β_1. When the arrival times of the events from $N_1(t)$, which are missing will be replaced by their corresponding expected values. For a given M, the MLE of the model parameters are obtained. Treating the resulting likelihood as a profile likelihood for β_1, the estimator of β_1 is obtained by maximizing it. Subsequently, information-theoretic criteria such as the AIC or the Bayesian Information Criterion (BIC) are used to select the optimal number and location of cut points.

We now derive the joint probability density function of the arrival times of NHPP. Let $\{N_1(t); t \geq 0\}$ be NHPP with intensity function $u_1(t)$ and $\tilde{\tau}_1, \tilde{\tau}_2, \ldots, \tilde{\tau}_n$ denote the arrival times of the first, second, and subsequent events from $N_1(t)$. Conditional on observing $N_1(\tau) = n$ events in the interval $(0, \tau]$, the joint probability density function of $\tilde{\tau}_1, \ldots, \tilde{\tau}_n$ can be written as

$$f_{\tilde{\tau}_1, \ldots, \tilde{\tau}_n | N_1(\tau) = n}(t_1, \ldots, t_n) = \frac{n!\, \beta_1^n}{\tau^{n\beta_1}} t_1^{\beta_1 - 1} \cdots t_n^{\beta_1 - 1}, \quad 0 < t_1 < t_2 < \cdots < t_n < \tau,$$

and zero otherwise.

Using this joint density, the conditional expectation of the jth arrival time, given $N_1(\tau) = n$, can be obtained as

$$E(\tilde{\tau}_j \mid N_1(\tau) = n) = \frac{n!\, \beta_1^n}{\tau^{n\beta_1}} \int_0^{t_2} \cdots \int_0^{t_n} \int_0^{\tau} t_1^{\beta_1 - 1} \cdots t_{j-1}^{\beta_1 - 1} t_j^{\beta_1 - 1} t_{j+1}^{\beta_1 - 1} \cdots t_n^{\beta_1 - 1}\, dt_1 \cdots dt_n.$$

After simplification, this expectation reduces to

$$E(\tilde{\tau}_j \mid N_1(\tau) = n) = \frac{\tau}{\left(1 + \frac{1}{j\beta_1}\right) \cdots \left(1 + \frac{1}{n\beta_1}\right)}.$$

When $\beta_1 = 1$, this is the case of a homogeneous Poisson process, the above expression simplifies to

$$E(\tilde{\tau}_j \mid N_1(\tau) = n) = \frac{j\tau}{n+1}.$$

The cut points are equally spaced over the interval $(0, \tau]$ in this scenario.

Similarly, for the second stress level, corresponding to the interval $(\tau, T]$, the cut-points $(\gamma_1, \ldots, \gamma_{Q-1})$ are similarly modeled as the arrival times of another NHPP $\{N_2(t); t \geq 0\}$, defined with a different intensity function $u_2(t) = \beta_2 t^{\beta_2 - 1}, \quad \beta_2 > 0$. Estimation of the lifetime model parameters $\lambda_{k,r}, \alpha_2$ and the NHPP parameter β_2 proceeds in the same manner as for the first stress level. Let $\tilde{\gamma}_1, \tilde{\gamma}_2, \ldots \tilde{\gamma}_n$ be the arrival times of the events from $N_2(T)$. Similarly, for a given number of cut points $N_2(T) = n$, the position of jth cut point will be

$$E(\tilde{\gamma}_j \mid N_2(T) = n) = \tau + \frac{T - \tau}{\left(1 + \frac{1}{j\beta_2}\right) \cdots \left(1 + \frac{1}{n\beta_2}\right)}.$$

In practice, the above method has been implemented as follows. For fixed numer of cut points (M, Q), we have obtained the MLEs of (β_1, β_2) and $(\lambda_{k,r}, \alpha_i)$. We have calculated this in two steps: first for fixed (β_1, β_2) we have computed the MLE of $(\lambda_{k,r}, \alpha_i)$ and then for fixed value of (M, Q) and $(\tau, T) = (6, 12)$, we have estimated the model parameters along with AIC and BIC for different choices of (β_1, β_2) with grid size 0.05. we have selected the optimal value of (β_1, β_2) based on lowest value of AIC and BIC. The grid search results for the cases with two, three, and four cut points are summarized graphically through heatmaps of AIC and BIC values over the (β_1, β_2) grid, which are presented in Figures 5, 6, and 7, respectively. We have noted the optimal values of (β_1, β_2) along with the location of cut points corresponding to the lowest AIC and BIC in Table 10. Using the cut-point locations from Table 10, we have plotted the empirical CDFs along with the fitted CDFs for two, three, and four cut points, as shown in Figure 8. These plots show that the fitted distributions closely follow the empirical CDF. Although for two cut points, the plot indicates that the proposed model provides an adequate fit to the data. However, by increasing the cut points to three and four, the corresponding AIC and BIC values do not decrease substantially. This is mainly due to the penalty term in the information criteria, which increases as more parameters are added to the model. Once two cut points are introduced, the model already captures the structure of the data more effectively, and further increases in the number of cut points lead only to marginal improvements in the likelihood, insufficient to offset the increased model complexity. Similar observations have been reported in the literature, where it is often noted that models with two to three cut points are generally sufficient to achieve a good fit (see Balakrishnan et al. (2016)[9], Goodman et al. (2011)[30], Murphy (1996)[8] and Samanta and Kundu (2023)[10]). In view of this, we restrict our attention to models with two, three, and four cut points in the present analysis. We have also reported the MLEs of the model parameters in Table 11, which correspond to the values reported in Table 10. Based on these results, the selected model achieves a satisfactory fit while avoiding unnecessary over parameterization.

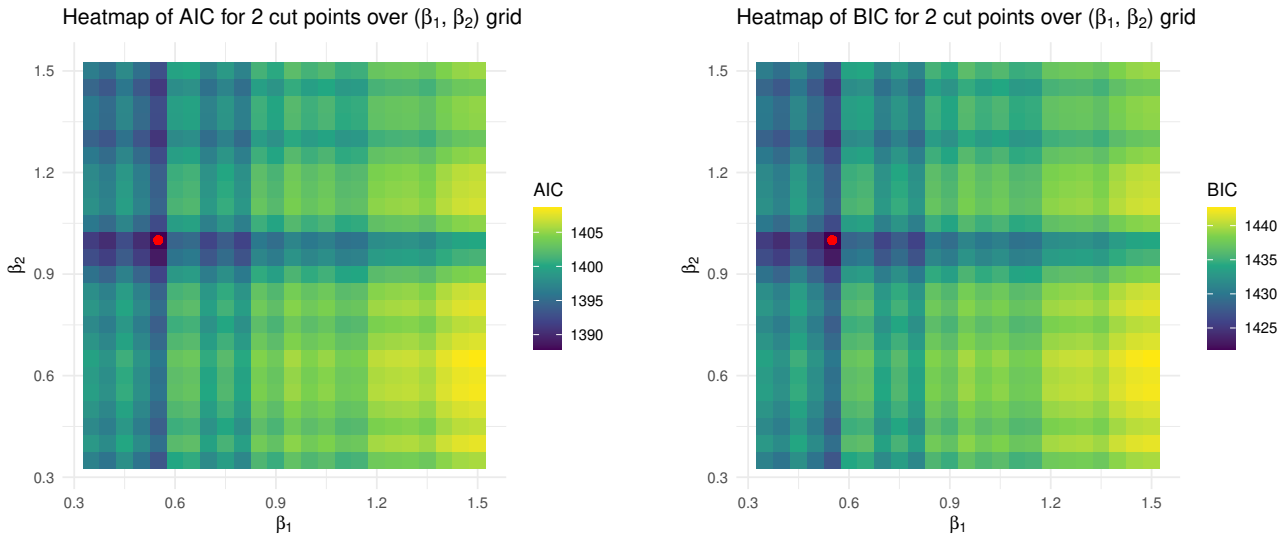

Figure 5: Heatmaps of AIC and BIC over the (β_1, β_2) grid for the two–cut-point model, with the red dot denoting the minimum AIC/BIC location

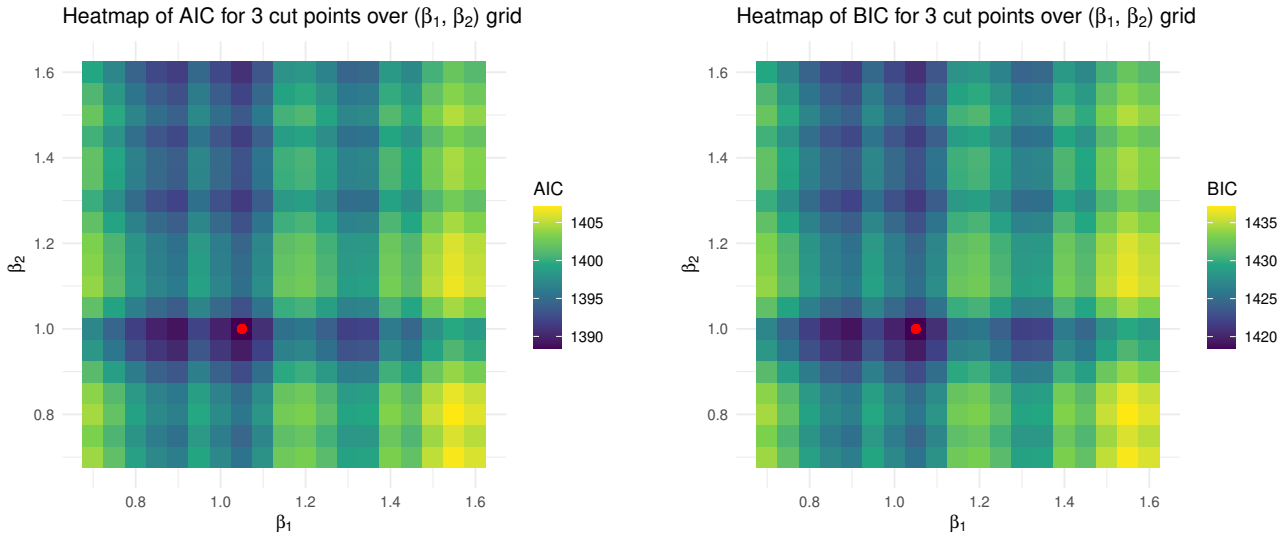

Figure 6: Heatmaps of AIC and BIC over the (β_1, β_2) grid for the three–cut-point model, with the red dot denoting the minimum AIC/BIC location

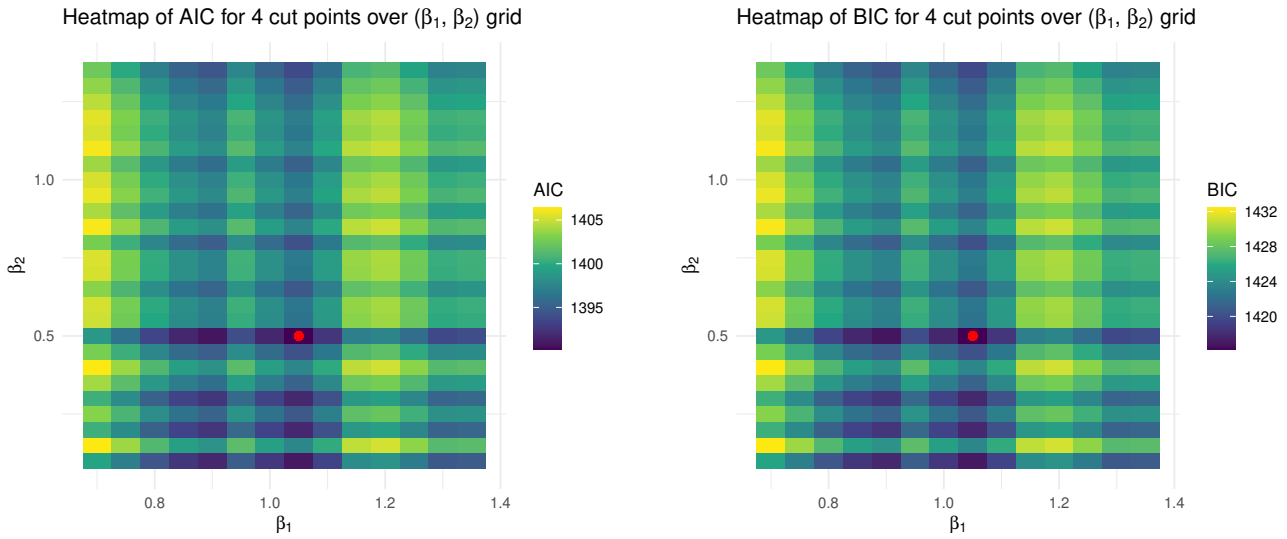

Figure 7: Heatmaps of AIC and BIC over the (β_1, β_2) grid for the four–cut-point model, with the red dot denoting the minimum AIC/BIC location

Table 10: Estimated locations of the cut points and the corresponding AIC and BIC values

(M, Q)	β_1	β_2	τ_1	τ_2	γ_1	γ_2	Log-likelihood	AIC	BIC
(2,2)	0.55	1	2.1291		9		-683.91	1387.81	1421.83
(3,2)	1.05	1	2.0818	4.0645	9		-682.19	1388.38	1429.21
(3,3)	1.05	0.5	2.0818	4.0645	7	9	-681.08	1390.17	1437.81

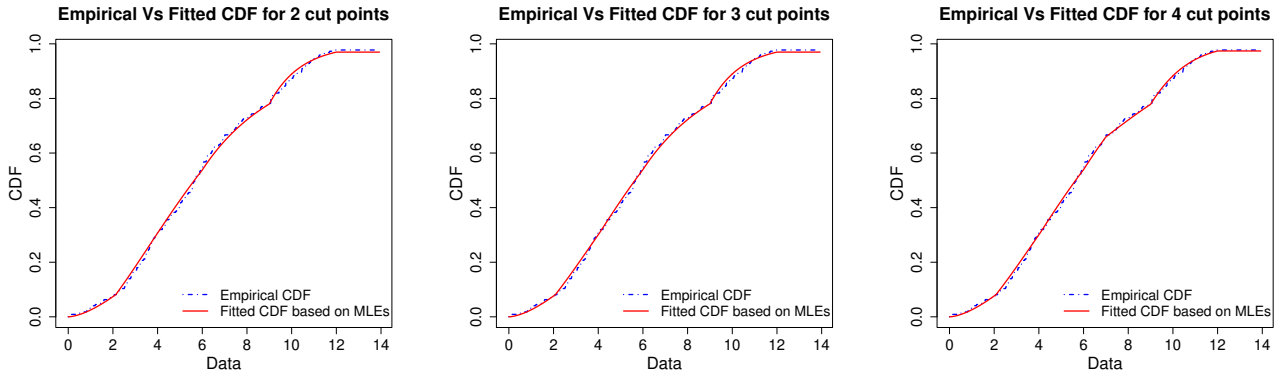

Figure 8: Plot of empirical versus fitted CDF based on MLEs of real dataset for different cut points

Table 11: MLE of the model parameters for the real dataset under optimal choices of cut points

(M, Q)	α_1	α_2	$\lambda_{1,1}$	$\lambda_{2,1}$	$\lambda_{1,2}$	$\lambda_{2,2}$	$\lambda_{1,3}$	$\lambda_{2,3}$	$\lambda_{1,4}$	$\lambda_{2,4}$	$\lambda_{1,5}$	$\lambda_{2,5}$	$\lambda_{1,6}$	$\lambda_{2,6}$
(2,2)	1.603	0.574	0.002	0.022	0.023	0.024	0.621	0.387	1.988	1.136				
(3,2)	1.608	0.574	0.002	0.023	0.026	0.018	0.018	0.031	0.621	0.387	1.988	1.136		
(3,3)	1.608	2.123	0.002	0.023	0.026	0.018	0.018	0.031	0.009	0.007	0.006	0.003	0.015	0.008

7 Conclusion

In this article, we propose a flexible semiparametric framework for analyzing simple step-stress ALT data in the presence of competing risks. The proposed model uses a piecewise monotone hazard functions, which allow failure rates to vary across time intervals and stress levels while maintaining a clear parametric interpretation within each interval. This structure offers greater modeling flexibility than fully parametric step-stress models and is particularly useful when the underlying failure behaviour changes over time. Also, the proposed framework is a natural generalization of the piecewise constant hazard function model. Both classical and Bayesian inferential procedures have been developed to estimate the model parameters. MLEs and their associated ACIs were obtained under the classical setup, while Bayes estimates along with symmetric and HPD credible intervals were constructed by assuming suitable prior distributions. The Bayesian computation was carried out efficiently using Gibbs sampling. The extensive simulation study clearly indicates that the proposed estimation procedures perform well in terms of average estimates, mean squared errors, interval lengths and coverage perentages, and the performance improves as the sample size increases. The practical applicability of the proposed methodology has been demonstrated through the analysis of a real competing risk dataset. The results show that the semiparametric model provides a good fit to the data and can capture complex time-dependent failure patterns that standard parametric models may not adequately address. We also compare the proposed model with the piecewise constant hazard model (with and without cut points) and the conventional Weibull step-stress model. The results demonstrate that the proposed framework provides greater flexibility in capturing failure behavior than these existing approaches. Overall, the proposed approach offers a reliable and effective alternative to commonly used parametric step-stress competing risk models. In this work, the number and locations of the cut points were assumed to be known. However, in real applications, these are typically unknown. A data-driven strategy based on information criteria such as AIC and BIC has also been employed to select the number and positions of cut points, which makes the approach practically implementable. Although the current study focuses on a simple step-stress setup with two competing risks, but the proposed framework can be extended to more general settings, including multiple stress levels, additional competing causes, and other advanced censoring schemes. Further investigation along these directions would be worthwhile for future research.

Funding

This work did not receive any financial support or funding.

Data Availability

The study used a publicly accessible dataset, which is cited within the manuscript.

Conflict of Interest

The authors declare that they have no conflicts of interest related to this work.

References

[1] Bagdonavičius, V., Cheminade, O., & Nikulin, M. (2004). Statistical planning and inference in accelerated life testing using the CHSS model. Journal of Statistical Planning and Inference, 126(2), 535-551.

[2] Miller, R., & Nelson, W. (2009). Optimum simple step-stress plans for accelerated life testing. IEEE Transactions on Reliability, 32(1), 59-65.

[3] Meeker, W. Q., Escobar, L. A., & Pascual, F. G. (2021). Statistical methods for reliability data. John Wiley & Sons.

[4] Sedyakin, N. M. (1966). On one physical principle in reliability theory. Techn. Cybernetics, 3, 80-87.

[5] Bhattacharyya, G. K., & Soejoeti, Z. (1989). A tampered failure rate model for step-stress accelerated life test. Communications in statistics-Theory and methods, 18(5), 1627-1643.

[6] Kateri, M., & Kamps, U. (2015). Inference in step-stress models based on failure rates. Statistical Papers, 56(3), 639-660.

[7] Kundu, D., & Ganguly, A. (2017). Analysis of step-stress models: existing results and some recent developments. Academic Press.

[8] Murphy, A. (1996). A piecewise-constant hazard-rate model for the duration of unemployment in single-interview samples of the stock of unemployed. Economics Letters, 51(2), 177-183.

[9] Balakrishnan, N., Koutras, M. V., Milienos, F. S., & Pal, S. (2016). Piecewise linear approximations for cure rate models and associated inferential issues. Methodology and Computing in Applied Probability, 18(4), 937-966.

[10] Samanta, D., & Kundu, D. (2023). Bivariate semi-parametric model: Bayesian inference. Methodology and Computing in Applied Probability, 25(4), 87.

[11] Ganguly, A., Mitra, D., Balakrishnan, N., & Kundu, D. (2024). A flexible model based on piecewise linear approximation for the analysis of left truncated right censored data with covariates, and applications to Worcester Heart Attack Study data and Channing House data. Statistics in Medicine, 43(2), 233-255.

[12] Pal, A., Samanta, D., & Kundu, D. (2025). A semiparametric approach for simple step-stress model. Test, 34(1), 91-124.

[13] Prajapati, D., & Kundu, D. (2025). On Semi-Parametric Progressive Censoring: D. Prajapati and D. Kundu. Statistics and Computing, 35(6), 204.

[14] Cox, D. R. (1959). The analysis of exponentially distributed life-times with two types of failure. Journal of the Royal Statistical Society Series B: Statistical Methodology, 21(2), 411-421.

[15] David, H. A., & Moeschberger, M. L. (1978). The theory of competing risks. London, U.K.: Griffin.

[16] Beltrami, J. (2015). Exponential competing risk step-stress model with lagged effect. Int. J. Math. Stat, 16(1), 1-24.

[17] Balakrishnan, N., & Han, D. (2008). Exact inference for a simple step-stress model with competing risks for failure from exponential distribution under Type-II censoring. Journal of Statistical Planning and Inference, 138(12), 4172-4186.

[18] Liu, X., & Qiu, W. S. (2011). Modeling and planning of step-stress accelerated life tests with independent competing risks. IEEE Transactions on Reliability, 60(4), 712-720.

[19] Zhang, C., Shi, Y., & Wu, M. (2016). Statistical inference for competing risks model in step-stress partially accelerated life tests with progressively Type-I hybrid censored Weibull life data. Journal of computational and applied mathematics, 297, 65-74.

[20] Samanta, D., Gupta, A., & Kundu, D. (2019). Analysis of Weibull step-stress model in presence of competing risk. IEEE Transactions on Reliability, 68(2), 420-438.

[21] Peña, E. A., & Gupta, A. K. (1990). Bayes estimation for the Marshall–Olkin exponential distribution. Journal of the Royal Statistical Society Series B: Statistical Methodology, 52(2), 379-389.

[22] Kundu, D., & Pradhan, B. (2011). Bayesian analysis of progressively censored competing risks data. Sankhya B, 73(2), 276-296.

[23] Kinderman, A. J., & Monahan, J. F. (1977). Computer generation of random variables using the ratio of uniform deviates. ACM Transactions on Mathematical Software (TOMS), 3(3), 257-260.

[24] Congdon, P. (2014). Applied bayesian modelling. John Wiley & Sons.

[25] Dukers, N. H., Renwick, N., Prins, M., Geskus, R. B., Schulz, T. F., Weverling, G. J., & Goudsmit, J. (2000). Risk factors for human herpesvirus 8 seropositivity and seroconversion in a cohort of homosexula men. American journal of epidemiology, 151(3), 213-224.

[26] Xiridou, M., Geskus, R., De Wit, J., Coutinho, R., & Kretzschmar, M. (2003). The contribution of steady and casual partnerships to the incidence of HIV infection among homosexual men in Amsterdam. Aids, 17(7), 1029-1038.

[27] Putter, H., Fiocco, M., & Geskus, R. B. (2007). Tutorial in biostatistics: competing risks and multi-state models. Statistics in medicine, 26(11), 2389-2430.

[28] Geskus, R. B., González, C., Torres, M., Del Romero, J., Viciana, P., Masiá, M., & CoRIS-HPV Study Group. (2016). Incidence and clearance of anal high-risk human papillomavirus in HIV-positive men who have sex with men: estimates and risk factors. Aids, 30(1), 37-44.

[29] Alotaibi, R., Almetwally, E. M., Ghosh, I., & Rezk, H. (2024). Statistical inference of a step-stress model with competing risks under time censoring for alpha power exponential distribution. Journal of Radiation Research and Applied Sciences, 17(1), 100771.

[30] Goodman, M. S., Li, Y., & Tiwari, R. C. (2011). Detecting multiple change points in piecewise constant hazard functions. Journal of applied statistics, 38(11), 2523-2532.